Scripta Materialia 107 (2015) 67–70

Contents lists available at ScienceDirect

Scripta Materialia

journal homepage: www.elsevier.com/locate/scriptamat

Microstructural vortex formation during cyclic sliding of Cu/Au multilayers

Zhao-Ping Luo [a], Guang-Ping Zhang [b], Ruth Schwaiger [a,*]

[a] Institute for Applied Materials, Karlsruhe Institute of Technology (KIT), 76021 Karlsruhe, Germany
[b] Shenyang National Laboratory for Materials Science, Institute of Metal Research, Chinese Academy of Sciences, 110016 Shenyang, China

ARTICLE INFO

Article history:
Received 18 April 2015
Revised 19 May 2015
Accepted 20 May 2015
Available online 28 May 2015

Keywords:
Multilayers
Deformation structure
Scratch test
Kelvin–Helmholtz instability

ABSTRACT

Cu/Au multilayers with individual layer thickness of 100 nm were deformed by cyclic sliding using a nanoindenter. With increasing cycle number, a distinct sequence of changes was observed, from uniform thinning through formation of waviness and vortices until finally a mechanically mixed structure developed. Fluid-like behavior is observed and gradients of strain and strain rate are suggested to initiate the evolution of vortices driving the mechanical mixing of the layers.

Nanoscale metallic multilayers have long been known for their high strength and hardness [1–3] with layer thickness and interface structure as the controlling factors [3–5]. The importance of metallic multilayers in the context of fatigue [6–8] and wear [9,10] has also been demonstrated. Both the fatigue strength [7,8] and wear resistance [9] were observed to increase with decreasing layer thickness. Nanoscale Cu–Ni multilayer coatings very effectively suppressed fatigue crack initiation and showed evidence of reduced accumulated plasticity compared to monolithic coatings [6]. Recently it was suggested that a nanolayered structure that formed during wear testing of $Cu_{90}Ag_{10}$ alloys – in combination with Ag acting as a solid lubricant – was responsible for reduced wear rates [11]. Considering the high thermal stability of Cu–Nb multilayers [12] and their resistance to radiation damage [13], multilayers represent excellent candidates for applications under extreme loading and temperature conditions. However, in order to understand and exploit these excellent properties, the role of the interface in large strain deformation, plastic deformation mechanisms and deformation microstructures need to be investigated in greater detail for different types of interfaces.

In the research presented here, cyclic sliding experiments on Cu/Au multilayers were conducted using a nanoindenter with the goal to study the evolution of the microstructure of a miscible face-centered cubic multilayer system under severe deformation. For ductile materials, it was illustrated that severe plastic deformation is introduced during sliding wear experiments with shear strains exceeding 10 [14]. Using a nanoindenter, it is possible to locally apply large plastic strains underneath a well-defined contact in order to gain a fundamental understanding of the deformation processes, which is important in the context of micro- and nanomechanics but may also add to our understanding of macroscopic wear. For example, sliding contact has been suggested as a method to estimate yield strength and strain hardening of small-volume materials [15] and has been used to investigate the small-scale frictional sliding of nanotwinned Cu [16].

For our study, Cu/Au multilayers were deposited on single-crystalline Si (001) substrates (thickness 500 μm) by radio-frequency magnetron sputtering. The purity of the Cu and Au targets was 99.999 at.% and 99.95 at.%, respectively, and the deposition rate was 0.3 nm/s. The total thickness of the multilayer film was ~1 μm, while the nominal individual layer thickness was 100 nm for both Cu and Au layers with interfaces that were not compositionally sharp [17]. The Au layer was deposited as the top layer to minimize the effects of sample surface oxidation. X-ray diffraction indicated that the layer interface had a Cu{1 1 1} // Au{1 1 1} relationship [18]. Sliding experiments were conducted using a Nanoindenter G200 XP (Agilent Technologies, USA) with a spherical diamond tip of 16.7 μm diameter. A constant normal load of 10 mN was applied resulting in an initial penetration of ~50 nm while the sample stage was moved back and forth at a rate of 5 μm/s over a distance of 100 μm. Tests with up to

* Corresponding author. Tel.: +49 721 608 24878.
E-mail address: ruth.schwaiger@kit.edu (R. Schwaiger).

http://dx.doi.org/10.1016/j.scriptamat.2015.05.022
1359-6462/

1000 cycles were performed with one back and forth movement defined as one sliding cycle. The experiments were conducted at room temperature in air with relative humidity of 50%. Prior to every experiment, the nanoindenter tip was cleaned with propanol. Although we expect changes of the tip shape, careful inspection by scanning electron microscopy (SEM) after every test indicated no visible changes of the tip. The microstructure underneath the sliding tracks was investigated by SEM (Nova 200 NanoLab, FEI, USA) and transmission electron microscopy (TEM). TEM samples were prepared by focused ion beam (FIB) milling using the standard lift-out technique and investigated in a Philips CM-30 operated at 300 kV and a FEI Tecnai F20 operated at 200 kV.

Fig. 1a shows the original morphology of the Cu/Au multilayer film. As determined from cross-sectional SEM images, the average layer thickness of Cu and Au is 110.0 ± 3.2 nm and 101.6 ± 11.6 nm, respectively, and the total film thickness 1062.3 ± 26.9 nm. The top or first layer at the specimen surface is Au, while the bottom layer, i.e. tenth layer, is Cu. Significant microstructural changes were observed after the sliding experiments (Figs. 1 and 2). After ten cycles, thinning of the first two layers was observed (Fig. 1b) accompanied by grain coarsening (Fig. 3a and b). After 20 cycles, further thinning had occurred while at the same time the interfaces started to exhibit pronounced waviness (Fig. 1c). After 100 cycles, deformation extended over five layers and vortices were observed (Figs. 1d and 2). Such a structure resembles the flow patterns that are expected in fluid flow under a Kelvin–Helmholtz instability, which can occur in the shear layer between two fluids in the presence of a velocity gradient and results in fluid turbulence and mixing [19]. With further increase in cycle numbers, more layers were involved in the plastic deformation and the vortices became more pronounced (Fig. 1e). Finally, the layer structure disappeared completely in the deformed zone (Fig. 1f). Similarities to Kelvin–Helmholtz instabilities, vortex formation and material mixing at the sliding interface were also revealed previously by simulations of sliding of crystalline and amorphous solids [20,21]. While Fig. 1 shows the cross sections perpendicular to the sliding direction, Fig. 2 depicts parallel ones in the center of the sliding track showing the same mixing behavior indicating isotropic microstructural evolution.

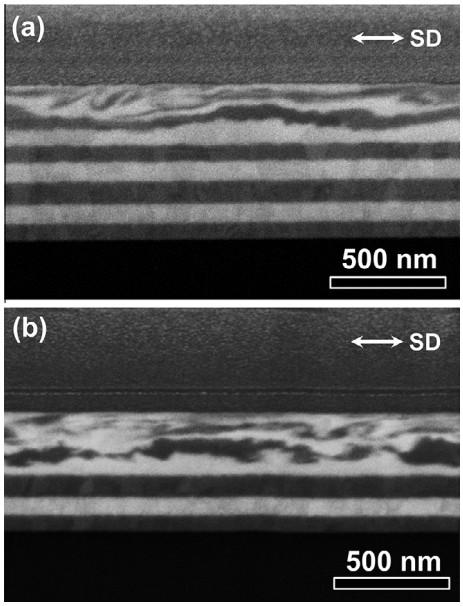

Figure 2. SEM images of the sliding tracks along the sliding direction after (a) 50 and (b) 500 cycles.

The changes of the individual layer thicknesses after different cycle numbers were quantified using SEM (Table 1). Typically, the measured layer thicknesses vary within ±5% over the sample, and thus only a change $\geqslant$5% is considered as a thickness change resulting from sliding. After the first cycle, the first two layers exhibit an obvious thickness reduction, while further below, no change in layer thickness was observed. After ten cycles, the top three layers were involved in the deformation; then, deformation spreads to the other layers with increasing cycle numbers. Layers 1–4 are heavily deformed after 50 cycles and their thickness can no longer be determined.

Our TEM investigation clearly shows that the grain size had increased significantly in the deformed layers prior to the vortex formation, whereas no changes were observed in the undeformed layers (Fig. 3a and b).

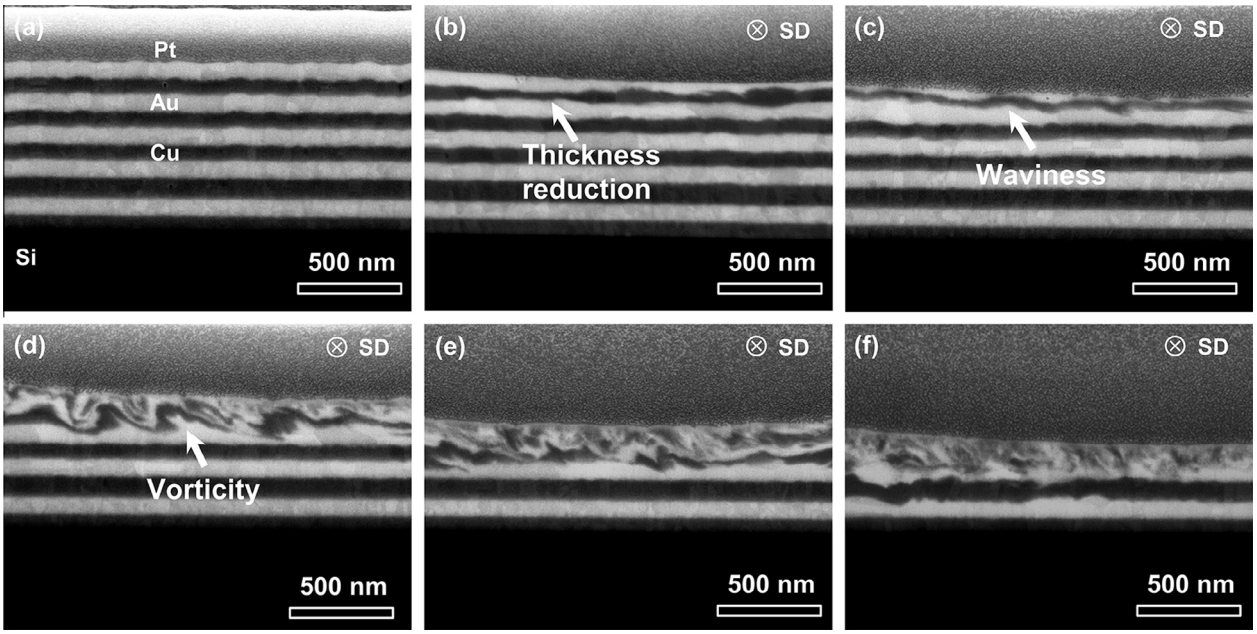

Figure 1. SEM images (at 52° sample tilt) of FIB-prepared cross sections perpendicular to the sliding direction (SD) of (a) the undeformed Cu/Au multilayer on Si and (b)–(f) the sliding tracks after 10, 20, 100, 500, and 1000 cycles. After (b) layer thinning and (c) waviness of the layers and grain coarsening, (d–f) a vortex structure was observed.

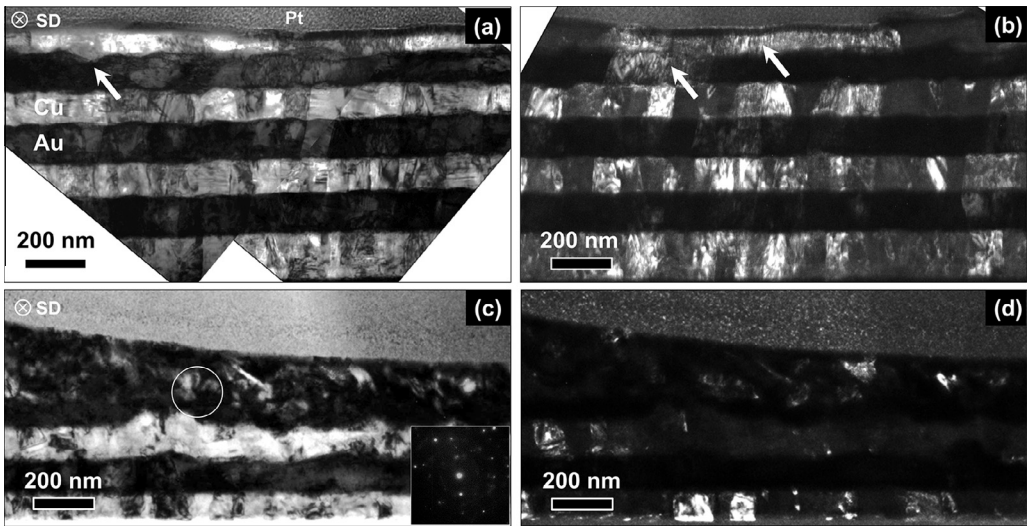

Figure 3. (a) TEM bright-field and (b) dark-field images of Cu/Au multilayers after 10 cycles. The top two layers were thinned and waviness increased (indicated by arrow in (a)). Grain growth was observed in the 2nd and 3rd layers, as indicated in (b). (c) Bright-field and (d) dark-field TEM images after 1000 cycles. The inset in (c) shows a selected area diffraction image of the circled region, indicating the deformed region is nanocrystalline.

Table 1
Thickness reduction $\varepsilon = (\lambda - \lambda^*)/\lambda$, with λ and λ^* as the layer thicknesses of the individual layers before and after sliding as function of cycle number. The layer thickness determined from SEM images of FIB cross sections has a typical 5% variation over the sample; thus, $\varepsilon < 5\%$ is shown as "0". The indicator "–" means the individual layer thickness could not be identified because of layer mixing.

Layers	1 cycle	10 cycles	50 cycles	200 cycles	500 cycles	1000 cycles
1 (Au)	5.69 ± 4.50%	35.09 ± 13.05%	–	–	–	–
2 (Cu)	13.80 ± 5.94%	38.75 ± 14.16%	–	–	–	–
3 (Au)	0	4.52 ± 13.72%	–	–	–	–
4 (Cu)	0	0	–	–	–	–
5 (Au)	0	0	9.06 ± 7.88%	–	–	–
6 (Cu)	0	0	0	13.81 ± 11.86%	–	–
7 (Au)	0	0	0	4.96 ± 10.41%	17.88 ± 30.23%	–
8 (Cu)	0	0	0	0	0	23.22 ± 17.95%
9 (Au)	0	0	0	0	0	5.03 ± 17.48%
10 (Cu)	0	0	0	0	0	0

It is unlikely that frictional heating is responsible for the grain growth since the tip moved rather slowly over the surface. The maximum temperature is expected at the surface, while grain coarsening was also observed further below the surface with a sharp transition to the undeformed material, thus, indicating that the changes were deformation-driven. After 1000 cycles, a nanocrystalline structure was observed in the deformation zone (Fig. 3c and d), similar to the microstructural changes observed in unlubricated metal contacts, which are likely related to a low steady-state friction and wear behavior [22]. This was also reported for nanocrystalline metals and alloys [23–25], although the initially very small grain size evolved through grain coarsening into a stable nanocrystalline structure consisting of somewhat larger grains, while a steady-state of the friction coefficient or the wear rate was only observed for certain experimental conditions. For nanotwinned Cu [16], microstructural changes and variations of the grain size over the depth were observed below scratches; the microstructure approached a final grain size which was comparable for different initial microstructures and accompanied by a steady-state friction coefficient. In our experiments, however, the friction coefficient was not measured, but it is unlikely that a steady-state microstructure had developed within the 1000 cycles: as shown in Fig. 4, the penetration depth of the indenter tip into the film, which can be interpreted as a measure for the wear

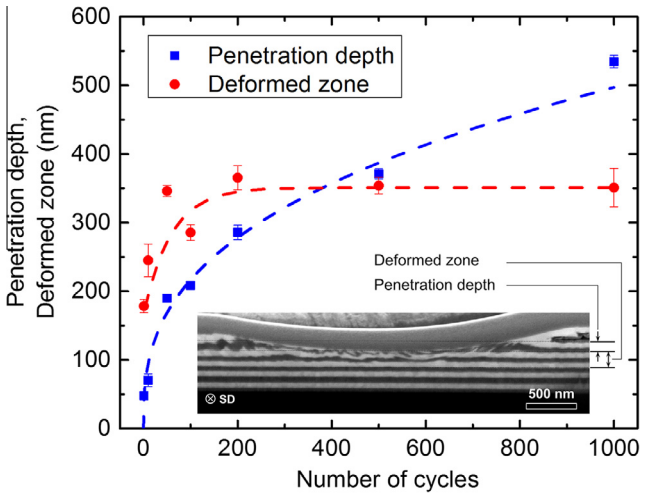

Figure 4. Penetration depth (blue) and thickness of the deformed zone (red) for different cycle numbers. The penetration depth increases continuously with increasing cycle number, while the thickness of the deformed zone was constant and ~350 nm after $N = 100$. (For interpretation of the references to color in this figure legend, the reader is referred to the web version of this article.)

volume, increased with increasing number of cycles indicating that the material removal was continuous. While the rate of the depth increase slowed down, this might well be an artifact and related to the presence of the substrate. The deformed sub-surface region, though, reached a constant thickness of ~350 nm after approximately 100 cycles (Fig. 4, red symbols), but the number of layers involved increased with increasing cycle numbers without reaching a steady state. The removed material formed folds along the edges of the sliding tracks (not shown here).

We observed different stages of the deformation process during cyclic sliding, i.e. thickness reduction, development of waviness, vortex formation and mechanical mixing. Depending on the individual layer thickness of multilayers, different deformation mechanisms are discussed in the literature, e.g. [26]. In the present study, the individual layers have an initial thickness of 100 nm, which is clearly in the dislocation-dominated size regime [26,27] with dislocations moving within the layers leading to layer thinning with increasing cycle numbers and accumulated plastic strain. During sliding, the layers thinned rapidly and entered a regime, in which also grain boundary mediated processes such as grain boundary sliding and grain rotation are expected to gain importance [28]. In previous studies, shear bands were observed in Cu/Au multilayers after indentation experiments [28,17] and elastic buckling assisted grain boundary sliding was suggested as the associated mechanism active in layers thinner than 50 nm [28]. However, the grain size in those films was significantly smaller compared to the grains after mechanical thinning (Fig. 3b). Here, no localized shear bands as in indentation were observed. Rather a continuous shear zone of constant thickness developed although more layers became consumed in the deformed zone; similarly as within the shear bands after indentation of Cu/Au multilayers [29], we observe clear evidence of interface instability and mixing of the two materials. A clear boundary appeared between the mixed structure and adjacent materials. This is consistent with the previous suggestion of mixed materials being brought by a flow process to a certain distance from the surface [14]. The multilayer structure experiences severe plastic deformation below the sliding contact and shear-induced mixing, which can be applied to induce mixing and homogenization of even immiscible elements [30] and was attributed to the motion of dislocations across interfaces [31]. In our samples, the steps at the interfaces between the layers (Fig. 3a) are very likely the result of dislocation plasticity and local dislocation pile-up against the interfaces [26] and appear to be the precursors for the vortex formation that enhances the mixing of the two materials. During the first few cycles, we observed co-deformation of the two layer types, but it is conceivable that there are differences in the plastic flow rate in the deformed Au and Cu layers. We thus have the conditions necessary to result in a Kelvin–Helmholtz instability [19–21], i.e. strain gradients underneath the sliding track and differences in the strain rate in the deformed layers.

The microstructures underneath the sliding tracks of Cu/Au multilayers were shown to exhibit a very distinct microstructural evolution. In cyclic sliding experiments using a nanoindenter, a deformation zone of constant thickness developed, while the rate of material removal did not reach a constant value within 1000 cycles. A sequence of layer thinning, grain coarsening and dislocation pile-up at the interfaces is suggested. The resulting waviness appears to be the precondition for a Kelvin–Helmholtz instability, which in combination with strain rate gradients results in vorticity-driven mechanical mixing and the formation of a nanocrystalline deformation layer. While strain rate gradients during sliding and fluid-like behavior have been suggested [21], this is to the best of our knowledge the most direct experimental observation supporting those suggestions.

This research was partially supported by the Helmholtz Association and the Chinese Academy of Sciences as a joint research group (HCJRG-217 and GJHZ1401). The support of Dr. Dimitri Litvinov (IAM, KIT) and Xi Li (IMR, CAS) with the TEM experiments is gratefully acknowledged.

References

[1] S.L. Lehoczky, J. Appl. Phys. 49 (1978) 5479.
[2] T. Tsakalakos, A.F. Jankowski, Annu. Rev. Mater. Sci. 16 (1986) 293.
[3] A. Misra, M. Verdier, Y.C. Lu, H. Kung, T.E. Mitchell, M. Nastasi, J.D. Embury, Scr. Mater. 39 (1998) 555.
[4] R.G. Hoagland, R.J. Kurtz, C.H. Henager Jr., Scr. Mater. 50 (2004) 775.
[5] J. Wang, A. Misra, Curr. Opin. Solid State Mater. Sci. 15 (2011) 20.
[6] M.R. Stoudt, R.E. Ricker, R.C. Cammarata, Int. J. Fatigue 23 (2001) S215.
[7] X.F. Zhu, G.P. Zhang, J. Phys. D Appl. Phys. 42 (2009) 055411.
[8] Y.C. Wang, A. Misra, R.G. Hoagland, Scr. Mater. 54 (2006) 1593.
[9] A.W. Ruff, D.S. Lashmore, Wear 151 (1991) 245.
[10] S.P. Wen, R.L. Zong, F. Zeng, Y. Gao, F. Pan, Wear 265 (2008) 1808.
[11] F. Ren, S.N. Arshad, P. Bellon, R.S. Averback, M. Pouryazdan, H. Hahn, Acta Mater. 72 (2014) 148.
[12] S. Zheng, I.J. Beyerlein, J.S. Carpenter, K. Kang, J. Wang, W. Han, N.A. Mara, Nat. Commun. 4 (2013) 1696.
[13] W.Y. Han, M.J. Demkowicz, N.A. Mara, E. Fu, S. Sinha, A.D. Rollett, Y. Wang, J.S. Carpenter, I.J. Beyerlein, A. Misra, Adv. Mater. 25 (2013) 6975.
[14] D.A. Rigney, Wear 245 (2000) 1.
[15] S.C. Bellemare, M. Dao, S. Suresh, Acta Mater. 58 (2010) 6385.
[16] A. Singh, N.R. Tao, M. Dao, S. Suresh, Scr. Mater. 66 (2012) 849.
[17] G.P. Zhang, Y. Liu, W. Wang, J. Tan, Appl. Phys. Lett. 88 (2006) 013105.
[18] Y.P. Li, X.F. Zhu, B. Wu, W. Wang, G.P. Zhang, J. Mater. Res. 24 (2009) 728.
[19] S.A. Thorpe, J. Fluid Mech. 46 (1971) 299.
[20] H.J. Kim, S. Karthikeyan, D. Rigney, Wear 267 (2009) 1130.
[21] D.A. Rigney, S. Karthikeyan, Tribol. Lett. 39 (2010) 3.
[22] D.A. Rigney, J.P. Hirth, Wear 53 (1979) 345.
[23] S.V. Prasad, C.C. Battaile, P.G. Kotula, Scr. Mater. 64 (2011) 729.
[24] H.A. Padilla II, B.L. Boyce, C.C. Battaile, S.V. Prasad, Wear 297 (2013) 860.
[25] T.J. Rupert, C.A. Schuh, Acta Mater. 58 (2010) 4137.
[26] A. Misra, J.P. Hirth, R.G. Hoagland, Acta Mater. 53 (2005) 4817.
[27] A. Misra, J.P. Hirth, H. Kung, Philos. Mag. A 82 (2002) 2935.
[28] Y.P. Li, X.F. Zhu, G.P. Zhang, J. Tan, W. Wang, B. Wu, Philos. Mag. 90 (2010) 3049.
[29] Y.P. Li, J. Tan, G.P. Zhang, Scr. Mater. 59 (2008) 1226.
[30] E. Ma, M. Atzmon, Mater. Chem. Phys. 39 (1995) 249.
[31] S.N. Arshad, T.G. Lach, M. Pouryazdan, H. Hahn, P. Bellon, S.J. Dillon, R.S. Averback, Scr. Mater. 68 (2013) 215.